

Real-Time Volumetric-Semantic Exploration and Mapping: An Uncertainty-Aware Approach

Rui Pimentel de Figueiredo, Jonas le Fevre Sejersen, Jakob Grimm Hansen, Martim Brandão and Erdal Kayacan

Abstract—In this work we propose a holistic framework for autonomous aerial inspection tasks, using semantically-aware, yet, computationally efficient planning and mapping algorithms. The system leverages state-of-the-art receding horizon exploration techniques for next-best-view (NBV) planning with geometric and semantic segmentation information provided by state-of-the-art deep convolutional neural networks (DCNNs), with the goal of enriching environment representations. The contributions of this article are threefold, first we propose an efficient sensor observation model, and a reward function that encodes the expected information gains from the observations taken from specific view points. Second, we extend the reward function to incorporate not only geometric but also semantic probabilistic information, provided by a DCNN for semantic segmentation that operates in real-time. The incorporation of semantic information in the environment representation allows biasing exploration towards specific objects, while ignoring task-irrelevant ones during planning. Finally, we employ our approaches in an autonomous drone shipyard inspection task. A set of simulations in realistic scenarios demonstrate the efficacy and efficiency of the proposed framework when compared with the state-of-the-art.

I. INTRODUCTION

This paper is focused on developing autonomous navigation, and mapping solutions for vision-based exploration and mapping of shipyard scenarios using unmanned aerial vehicles (UAVs). Inspection of a single vessel is costly, time consuming, and demanding as it requires manually categorizing damages and paint deterioration from low quality pictures. It is also risky since it has to be performed by human climbers through the use of scaffolding’s and mobile cranes. The use of UAVs offers a more cost effective and safer solution, since it avoids the need of direct intervention by human operators. We propose a solution for autonomous exploration and mapping using a single UAV, that combines probabilistic semantic-metric probabilistic measures fused in an efficient octogrid map representation, that are used by a fast geometric and semantically aware NBV planning algorithm, to efficiently reconstruct and label all objects.

The main contributions of this work are as follows:

- 1) An efficient probabilistic observation model for depth and semantic information provided by consumer grade RGB-D sensors and state-of-the-art DCNNs for 2D scene semantic segmentation.

R. Figueiredo, J. Sejersen, J. Hansen, E. Kayacan are with Artificial Intelligence in Robotics Laboratory (AiR Lab), the Department of Electrical and Computer Engineering, Aarhus University, 8000 Aarhus C, Denmark {jonas.le.fevre,rui,erdal} at ece.au.dk M. Brandão is with King’s College London (KCL), London, UK martim.brandao at kcl.ac.uk

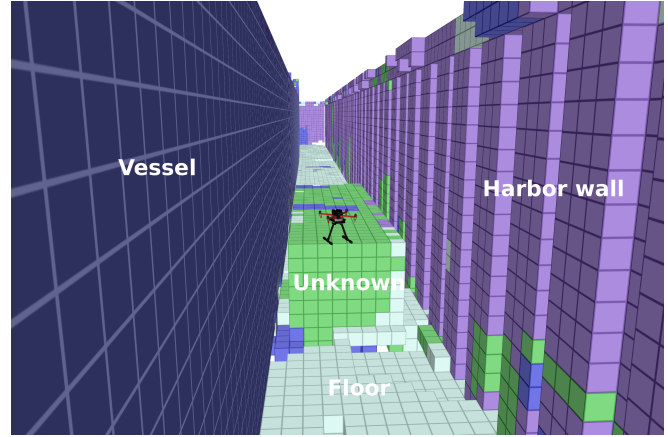


Fig. 1: A volumetric-semantic mapping representation of a simulated live-mission of an autonomous drone shipyard inspection task obtained using our volumetric and semantically uncertainty-aware receding horizon path planner.

- 2) A probabilistic mapping formulation that allows Bayesian fusion of volumetric and semantic information in a memory-efficient 3D octogrid structure.
- 3) A real-time, receding-horizon probabilistic path planning approach, that considers both geometric and semantic probabilistic information for planning, using rapidly-exploring random trees (RRTs). Our method is flexible and allows biasing exploration towards specific object classes.
- 4) A thorough evaluation of the advantages of our semantically-guided mapping approach when compared with the state-of-the-art in a realistic simulation environment.

The rest of this article is organized as follows: first, in Section II, we overview in detail the literature on semantic and geometric environment representations as well as NBV planning algorithms for autonomous mapping and robotics applications. Then, in Section III we describe the proposed methodologies for autonomous drone inspection tasks. The results Section IV evaluates the proposed strategies for autonomous mapping and navigation, in a realistic simulation shipyard environment. Finally, in Section V, some conclusions are drawn from this study and suggestions for future research are proposed.

II. RELATED WORK

In this section we overview the state-of-the-art on environment representations, and active perception algorithms for autonomous localization and mapping, used in robotics applications.

A. Map representations

The most common metric mapping representation in the literature is called probabilistic 3D occupancy grids. Such maps represent the environment as a block of cells, each one having a binary state (either occupied, or free). They are popular in the robotics community since they simplify collision checking and path planning, access is fast and memory use can be made efficient through octrees [1].

Semantic representations typically extend metric representations such as images and grids with a semantic layer, and rely on segmentation methods. Methods for 2D image semantic segmentation deal with the task of associating each pixel of an image as belonging to one of a set of different known classes. State-of-the-art methods for image segmentation are based on deep neural network architectures [2], [3] that learn from large annotated datasets to regress from 2D images to object masks that encode the layout of input object's. The Bilateral Segmentation Network (BiSeNet) [4], offers a way of balancing effectively the trade-off between speed and accuracy. BiSeNet [4] first comprises a spatial path with a small stride to preserve spatial information and generate high-resolution feature maps, and a context path with a fast down-sampling mechanisms for the generation of high resolution receptive fields. These are efficiently merged, using a feature fusion module. In this work we use BiSeNet for image semantic-segmentation, because it is compact, fast, robust [5], and easy to use, making in suitable for remote sensing applications running on embedded systems (e.g. UAVs) with low budget computational specifications.

B. Active perception

In this paper we tackle the problem of actively controlling the viewpoint(s) of a sensor(s) to improve task performance, which is of the utmost importance in robotics applications [6].

1) *Next-best-view planning*: NBV planning has been widely studied by the robotics community and plays a role of primordial importance on object reconstruction [7], autonomous mapping [8], and safe navigation [9] tasks, to name a few. Existing NBV approaches [10] belong to one of two main categories: frontier-based and information-driven planning. Frontier-based planners [11] guide the robot to boundaries between unknown and free space, which implicitly promotes exploration. Information-driven methods rely on probabilistic environment representations, and select the views that maximize expected information gains [10] by back-projecting probabilistic volumetric information on candidate views via ray casting. One approach to the problem is to incrementally compute and target a sensor at the NBVs according to some criteria (e.g. maximize 3D reconstruction quality). Instead of just considering the entropy, [8] proposes

a set of extensions to [12]'s information gain definition, including the incorporation of visibility probability as well as the likelihood of seeing new parts of the object [9]. Incremental sampling techniques (i.e. random tree sampling) [13], [14] sample the view space in a tree manner, using RRTs methods. Since taking all the possible views into consideration is computationally intractable, RRT-based approaches consider only a subset of possible views at each planning step. The tree is randomly expanded throughout the exploration space, and each branch forms a group of random subbranches. The quality of each branch is determined according to some criteria (e.g. by the amount of unmapped space that can be explored [15], [16]), and a receding-horizon approach is used at each planning step, until complete exploration of the environment is achieved.

III. METHODOLOGIES

In the rest of this section we describe the proposed system and methodologies for active exploration and semantic-metric mapping of man-made infrastructures.

A. System overview

The proposed drone system for autonomous inspection consists of a forward-facing camera, inertial measurement unit (IMU), and an altimeter. Our navigation system relies on an off-the-shelf simultaneous localization and mapping (SLAM) system with loop closing and relocalization capabilities [17], which is fed with RGB-D and IMU measurements, for improved robustness on self-motion tracking performance [18].

B. Probabilistic volumetric-semantic occupancy mapping

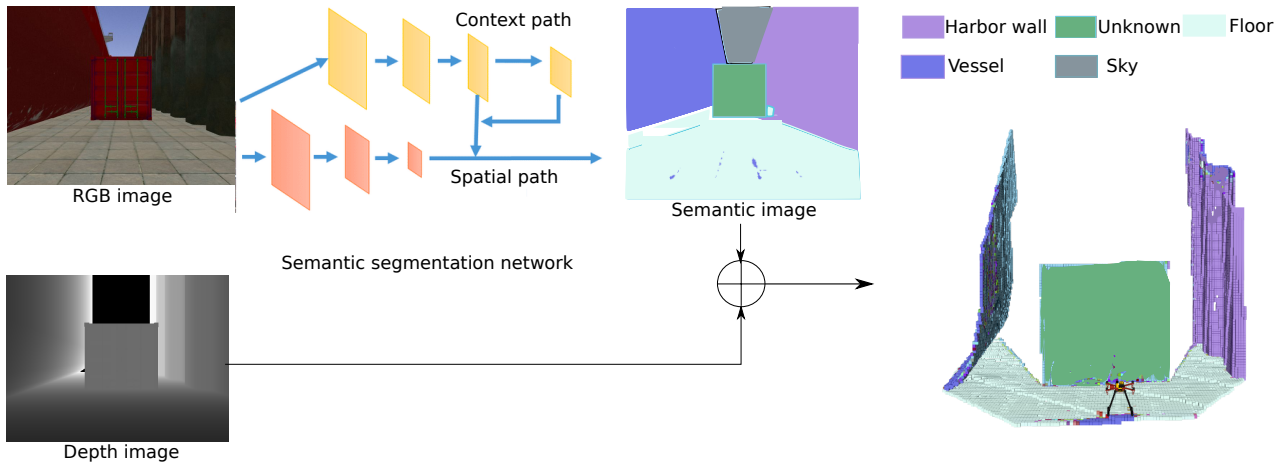
We consider an octomap representation, defined as a 3D uniform voxel grid structure that encloses the workspace around the robot, represented by $m = \{m_i\}$, where each voxel $m_i = \{m_i^o, m_i^s\}$ with $m_i^o \in \{0, 1\}$ being a binary random variable representing its occupancy, and $m_i^s \in \{1, \dots, K_c\}$ a semantic variable representing its object class. We use recursive Bayesian volumetric mapping [19] to sequentially estimate the posterior probability distribution over the map, given sensor measurements $z_{1:t} = \{z_{1:t}^o; z_{1:t}^s\}$ and sensor poses $p_{1:t}$ obtained through the robot kinematics model and an off-the-shelf SLAM module, from time 1 to t

$$P(m|z_{1:t}, p_{1:t}) = \prod_i P(m_i|z_{1:t}, p_{1:t}) \quad (1)$$

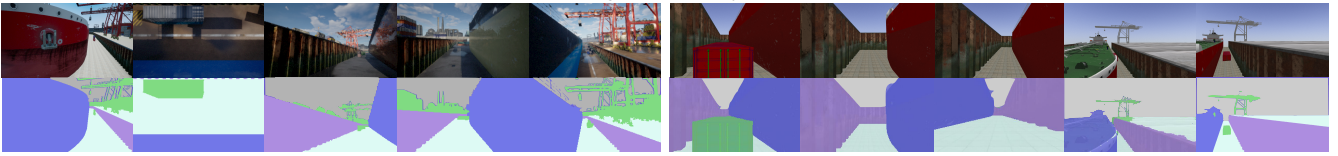
assuming the occupancy of individual cells are independent. Filtering updates can be recursively computed in log-odds space [20] to ensure numerical stability and efficiency.

C. 3D semantic segmentation

Our method for semantic segmentation relies on a DCNN encoder-decoder segmentation network, named BiSeNet [4]. BiSeNet receives RGB or grayscale images as input, encodes the image information, then decodes it again, and outputs a probability distribution over the known object categories for each pixel (u, v) .



(a) 3D semantic segmentation system architecture



(b) AirSim

(c) Gazebo

Fig. 2: (a) Proposed architecture for 3D semantic segmentation. (b) and (c) Top: sample training (b) and testing (c) images collected in Unreal Engine and Gazebo, respectively. Bottom: labelled (b) and inferred (c) images including ship (violet), sky (grey), floor (light blue), harbor walls (purple), and unknown harbor objects such as containers and cranes (green).

To obtain the 3D representation in real-time, we fuse the 2D semantic information provided by BiSeNet with depth measurements provided by consumer grade RGB-D cameras. For each pixel (u, v) belonging to an input image I , the network outputs a probability distribution $p^c(u, v) \in \mathcal{P}^{K_c}$ over the set of known classes \mathcal{C} , where K_c represents the number of known classes. For training the network we use the categorical Cross-Entropy loss function

$$CE = -\log \left(\frac{e^{s_p}}{\sum_j^C e^{s_j}} \right) \quad (2)$$

where s_j is the DCNN output score for the class $j \in \mathcal{C}$, and s_p the positive class.

At run-time, at each time instant t , the probability distributions over all classes and image pixels (i.e. probabilistic semantic image), obtained with BiSeNet, are merged with the corresponding depth image. We rely on a known extrinsic calibration parametric model, to obtain a semantic probabilistic point cloud (see Fig. 2a), where each point has a semantic probability distribution given by

$$P(z_{t,k}^s | I_t, p_t) \quad (3)$$

1) *Semantic dataset*: Supervised training of deep neural networks relies on the availability of large annotated data sets, hand-labeled in a laborious and time consuming manner, which may be impracticable for applications and machine learning tools, requiring large data sets. We train our BiSeNet model with synthetic data, generated in a realistic simulation environment to overcome the reality gap. The dataset used

for training our semantic segmentation network is generated using a combination of Unreal Engine 4 to create a realistic dock environment and AirSim [21] to extract the images and the corresponding labelled images, gathered by a multi-camera UAV (see Fig. 2). In order to increase the variability of the acquired dataset, shadows and illumination conditions are dynamically changed based on the simulated time of the day and weather conditions. For quantitatively testing the performance of our semantic segmentation networks, we have generated a dataset in Gazebo in a shipyard environment (see Table I).

D. Efficient probabilistic sensor fusion model

Our sensor depth noise model assumes that single point measurements $z_{t,k}^o$ are normally, independent and identically distributed (iid) according to

$$z_{t,k}^o | m, p_t \sim \mathcal{N}(z_{t,k}^{o*}; \Sigma_{t,k}^o) \quad (4)$$

with

$$\Sigma_{t,k}^o = \text{diag}(\sigma_{t,k}^l, \sigma_{t,k}^l, \sigma_{t,k}^a)$$

where $z_{t,k}^{o*}$ denotes the true location of the measurement and $\sigma_{t,k}^l$ and $\sigma_{t,k}^a$ represent the lateral and axial noise standard deviations, respectively. We assume that noise is predominant in the axial direction ($\sigma^a \gg \sigma^l$) which allows approximating the 3D covariance matrix by a 1D variance. For each measurement $z_{t,k}^o$, we then update the corresponding closest

TABLE I: Dataset used for training (AirSim), validating (AirSim) and testing (Gazebo) the proposed scene semantic segmentation network, for shipyard environments. The dataset specifications include the number of images and classes in each partition.

	# of Images	# Sky	# Floor	# Ship	# Harbor wall	# Unknown
Training data	49648	35353	45833	35281	28406	34951
Validation data	9930	7088	9177	7027	5587	6953
Test data	184	175	174	153	177	72

grid cell m_i as follows

$$P(m_{i,t}^o | z_{t,k}^o, p_t) \approx F_z \left(z_{t,k}^o + \frac{\delta}{2} \right) - F_z \left(z_{t,k}^o - \frac{\delta}{2} \right) \quad (5)$$

where δ represents the grid resolution and $F_z(\cdot)$ the cumulative normal distribution function of z , where the axial error standard deviation can be approximated by a simple quadratic model

$$\sigma_{t,k}^a \approx \lambda_a \|z_{t,k}^o\|^2 \quad (6)$$

with λ_a being a sensor specific scaling factor. All other cells belonging to the set of voxels traversed through ray casting (from the origin to end point z_i^o) are updated as being free with probability P_{free} . This is a reasonable approximation, considering that map resolution and sensory noise have the same order, while at the same time allowing to significantly reduce the amount of computation. The associated semantic measurements $z_{t,k}^s$, with probabilities given by $P(z_{t,k}^s | I_t, p_{t,k}) = \{P_1, \dots, P_{K_c}\}$ are updated independently, using

$$P(m_{i,t}^s | z_{t,k}^s, p_t) = \eta P(z_{t,k}^s | I_t, p_t) P(m_{i,t-1}^s | z_{1:t-1}^s, p_{1:t-1}) \quad (7)$$

where η is a normalizing constant.

E. Semantic-aware next-best-view planning

The proposed receding horizon NBV planner is based on the one of [16]. At each viewpoint, the planner generates a set of rays R that end if they collide against a physical surface or reach the limit of the map. For a given occupancy map representing the world m , the set of visible and unmapped voxels from configuration ξ_k is represented by $V(m, \xi_k)$. Every voxel $m_i \in V(m, \xi_k)$ lies in the unmapped exploration area and is visible by the sensor in configuration ξ_k (i.e. unoccluded and within the field of view). The expected information gain $G(n_k)$ for a given tree node n_k is the cumulative information gain collected from all nodes n_1, \dots, n_k , i.e. all nodes along the path from n_1 (the robot's current pose and RRT root) to n_k . This gain function is defined as

$$G(n_k) = G(n_{k-1}) + \left(\sum_{m_i \in V(m, \xi_k)} I_g(m_i) \right) e^{-\lambda \text{cost}(\sigma_{k-1}^k)} \quad (8)$$

where n_k is node k in the RRT, and the exponential is a weighting factor to favor low distance paths.

The original formulation of [16] models per-voxel infor-

mation gain I_g as

$$I_g(m_i) = \begin{cases} 1 & \text{if } P(m_i^o) = 0.5 \text{ (i.e. unknown)} \\ 0 & \text{otherwise (i.e. free or occupied)} \end{cases} \quad (9)$$

where $P(m_i^o)$ is the probability of cell i being occupied, i.e. they consider only volumetric information. Our method differs in the way information gain is defined. It leverages both the volumetric and semantic information entailed by each voxel. We model volumetric entropy at each voxel m_i as

$$H^o(m_i) = -P(m_i^o) \ln(P(m_i^o)) \quad (10)$$

and the semantic entropy as a sum over per-class entropy

$$H^s(m_i) = \sum_{k=1}^{K_c} H_k^s(m_i) \quad (11)$$

with per class-entropy $H_k^s(m_i)$ equal to

$$H_k^s(m_i) = -P(m_i^{s_k}) \ln(P(m_i^{s_k})) \quad (12)$$

where $P(m_i^{s_k})$ is the probability of cell i being of class k .

We propose two different probabilistic information gain formulations. The first formulation is agnostic to semantics and accounts only for the occupancy information the voxel provides, according to

$$I_g(m_i) = -H^o(m_i) \quad (13)$$

The second formulation incorporates semantic constraints as a weighted summation of the information gain per class, across all voxels:

$$I_g(m_i) = H^o(m_i) \sum_k \mathbf{w}_k^s H_k^s(m_i) \quad \sum_k \mathbf{w}_k^s = 1 \quad (14)$$

where $\mathbf{w}^s = [w_1^s, \dots, w_{K_c}^s]$ corresponds to a user specified weight vector, representing task-dependent class specific exploration biases. As in [16], the path which gets executed by the robot is picked by choosing the largest-gain node in the RRT, and executing the first segment of the path towards that node in a receding-horizon manner.

IV. EXPERIMENTS

In this section we conduct a set of experiments in a realistic simulation environment to assess the performance of the proposed holistic approach in a drone-aided shipyard inspection scenario. We use a quadcopter provided with a front-side RGB-D camera and an IMU. Our first goal was to assess the performance of the proposed pipeline on autonomous

mapping the shipyard environment. All experiments were run on an Intel® i7-10875H CPU with a GeForce RTX 2080 graphics card.

A. Semantic segmentation

a) *Semantic Segmentation Evaluation Metrics:* In order to access the performance of the image segmentation module, we rely on the pixel accuracy $P_{acc}(C)$ metric:

$$P_{acc}(c) = \frac{\#TP + \#TN}{\#TP + \#TN + \#FP + \#FN} \quad (15)$$

where true positive (TP), false positive (FP), true negative (TN) and false negatives (FN), represent pixels classified correctly as c , incorrectly as c , correctly as not c and incorrectly as not c , respectively.

We have quantitatively assessed the performance of our BiSeNet network model [4]) for an input size of 512×288 using the dataset described in Table I. Figure 3 shows the resulting confusion matrix on the test set (Gazebo), and demonstrates the network capability of learning to correctly classify different structures in the shipyard environment, with an overall accuracy of 97.7% on the test set (see Table II), without the need of domain randomization and adaptation techniques to bridge the gap between the two different domains.

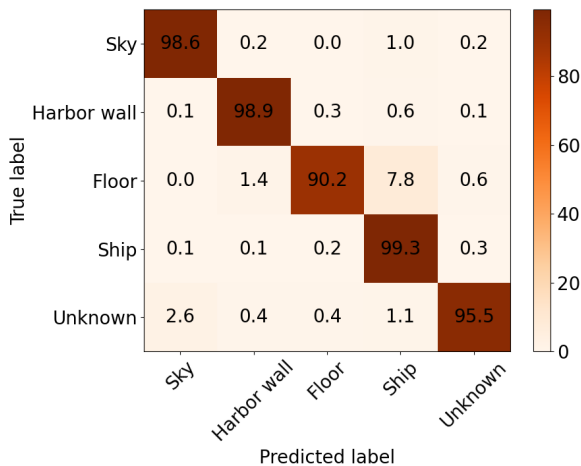


Fig. 3: Pixel confusion matrix for the semantic network, for 93% IoU score

TABLE II: Semantic segmentation network performance on the validation (AirSim) and test set (Gazebo).

	Overall Acc	Mean Acc	Mean IoU
Val	0.944	0.959	0.922
Test	0.977	0.965	0.930

B. Planning system evaluation

1) *Shipyards simulation scenario:* In order to be able to quantitatively and qualitatively measure the performance of

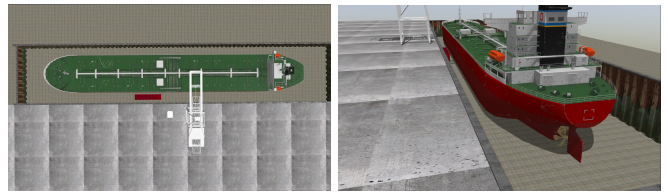


Fig. 4: Scenario used for evaluation in (Gazebo/ROS) simulation studies.

the proposed mapping and planning approaches, a realistic shipyard environment (see Fig. 4) was created using the Gazebo simulator [22]. The environment consists of a dry-dock measuring $145 \times 30 \times 8m$, containing a crane, a container and a dry dock. An intelligent active mapping algorithm should maximize task-related rewards, in this case information gathering, by focusing on rewarding viewing directions. We constrain the planner to output positions within this volume, since mapping and inspecting the top of the UAV is time-consuming and expensive (i.e. every hour in the dry dock is extremely costly).

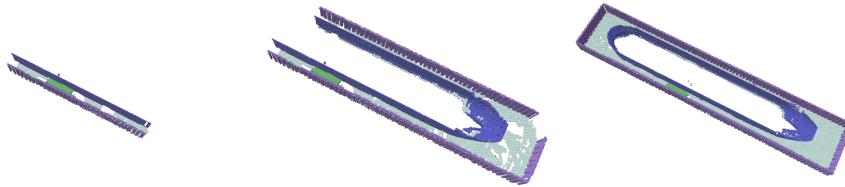
In all our experiments, the axial noise standard deviation scaling factor was set to $\lambda_a = 0.005$ and the occupancy probability threshold was set to $P_{occ} = 0.7$. In each experiment we let the observer collect $T = 2000$ observations (i.e. sense, plan and act iterations). Each experiment was repeated 10 times to average out variability in different simulations.

2) *Performance evaluation metrics:* We assess our NBV planning for active and autonomous exploration performance evaluation using the following metrics:

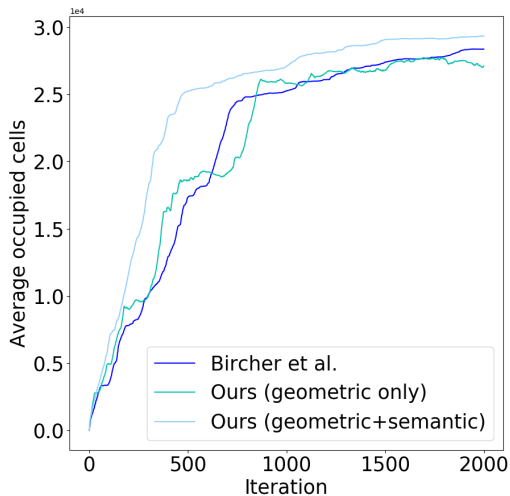
- the temporal entropy evolution, $\sum_{m_i \in m} H_t(m_i)$ which is a quality performance measure of the knowledge regarding the surrounding environment, gathered in the probabilistic volumetric map m , up to time t . When normalized by the number of planning steps it represents the temporal average global information gain per step, $\frac{1}{T} \sum_{t=1}^T \sum_{m_i \in m} H_t(m_i)$.
- amount of occupied cells (surface coverage) $\sum_{m_i \in m} \mathbf{1}(P_t(m_i))$ which is a measure of task-completeness and quantifies the surface covered during reconstruction, where P_{occ} represents a user specified probability threshold of the volume being occupied. When normalized by the number of reconstruction steps it represents the average surface coverage per step, $\frac{1}{T} \sum_{t=1}^T \sum_{m_i \in m} \mathbf{1}(P_t(m_i))$

Finally, we evaluate the computational performance (i.e. efficiency) of the methodologies by measuring sensor fusion and planning times.

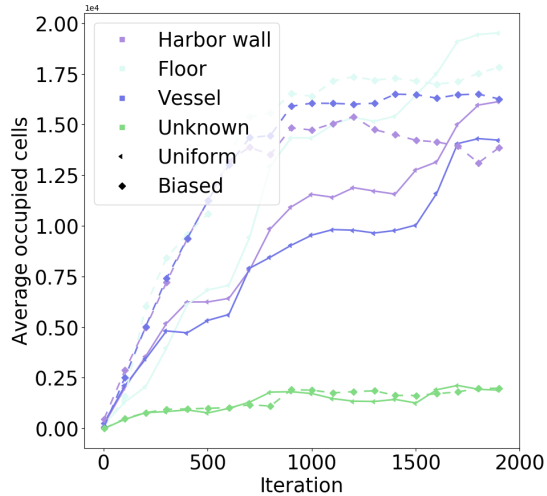
3) *Receding horizon geometric and semantic NBV planning:* The map resolution was set to $\delta = 0.4m$ to cope with the task requirements. The assessed map information was considered within the bounds of the motion and planning workspace. We compare the performance of our method to the state-of-the-art NBV planning approach of [15]. For assessing the advantages of incorporating semantics we considered two distributions for the class weights $C =$



(a) Example reconstruction evolution over NBV planning steps with our method. Octomap colored according to most likely semantics.



(b) Mapping occupancy.



(c) Per-class mapping occupancy.

Fig. 5: Mapping performance temporal evolution of our NBV planning in simulation. Each iteration includes planning, act, and sensing acquisition and fusion in the volumetric-semantic grid.

{Sky, Floor, Vessel, Harbor Wall, Unknown}. An unbiased uniform one

$$\mathbf{w}^s = [0.2, 0.2, 0.2, 0.2, 0.2] \quad (16)$$

to impose a purely geometric-driven exploration task, uninformed to semantics, and a biased one to bias exploration towards structures belonging to vessels

$$\mathbf{w}^s = [0.1, 0.1, 0.6, 0.1, 0.1] \quad (17)$$

Table III compares the computational performance of the different the baseline mapping [1] and planning [15] approaches. In this case although planning and mapping runs slower due to the computations involved in estimating the quality (probabilistic) of both geometric and semantic measurements and probabilistic fusion in a volumetric grid, it can still be used at reasonable rates for accurate sensor fusion. Furthermore, as can be seen in table IV, uncertainty aware planning improves mapping quality, due to the fact that previously seen map regions are on average attended more often, until uncertainty becomes negligible. As can be seen in Table V biasing exploration towards specific object classes improves task performance in terms of the mapping occupancy for the class of interest. Furthermore, as can be seen in Fig. 5c time-to-full coverage for a specific class (e.g. vessel) of interest is shorter when biasing exploration towards that class (e.g. convergence at around 750 steps).

TABLE III: Average computational times (ms) per iteration step

	Planning	Mapping
Bircher et al. [1]	70.3	43.3
Ours (geometric only)	82.2	41.2
Ours (geometric+semantics)	101.5	170.2

TABLE IV: Average information gain per iteration step.

	Iterations=2000
Bircher et al. [15]	72.19
Ours (geometric only)	82.2
Ours (geometric+semantics)	81.08

V. CONCLUSIONS

In this work we have proposed a holistic autonomous navigation framework for UAVs that incorporates probabilistic semantic-metric mapping representations for receding horizon NBVs planning. The navigation algorithm leverages both semantic and metric probabilistic gains, in order to decide where to move the UAV, to optimize visual data

TABLE V: Average occupancy per iteration step.

	Sky	Floor	Ship	Harbor wall	Unknown	Total
Bircher et al. [15]	-	-	-	-	-	52.3
Ours (geometric only)	-	-	-	-	-	55.6
Ours (geometric+semantic) (Uniform)	0	20.2	16	10	4	53.2
Ours (geometric+semantic) (Vessel Bias)	0	10.7	35.1	4.1	5	57.4

collection quality of objects of interest, in exploration tasks. We have introduced a probabilistic geometric and semantic observation model, and a mapping formulation that allows Bayesian fusion of volumetric and semantic information provided by consumer grade RGB-D sensors and state-of-the-art DCNNs for 2D scene semantic segmentation, in a memory efficient 3D octogrid structure. Then, we have proposed a real-time, receding-horizon probabilistic path planning approach, that considers both geometric and semantic probabilistic information for planning using RRTs. Our method is flexible and allows biasing exploration towards specifically known object classes. We have assessed the proposed framework on a realistic simulation environment (Gazebo), and demonstrated the benefits of the pipeline in a set of UAV-based inspection experiments. In the future we intend to evaluate our method in different scenarios, and extend the proposed approach with the ability to deal with multiple cameras [23], and schedule sensor acquisition such as to reduce computational load.

ACKNOWLEDGMENT

The authors would like to acknowledge the financial contribution from Smart Industry Program (European Regional Development Fund and Region Midtjylland, grant no.: RFM-17-0020). The authors would further like to thank Upteko Aps for bringing use-case challenges.

REFERENCES

- [1] A. Hornung, K. M. Wurm, M. Bennewitz, C. Stachniss, and W. Burgard, "Octomap: An efficient probabilistic 3d mapping framework based on octrees," *Autonomous Robots*, vol. 34, no. 3, pp. 189–206, 2013.
- [2] O. Ronneberger, P. Fischer, and T. Brox, "U-net: Convolutional networks for biomedical image segmentation," in *International Conference on Medical image computing and computer-assisted intervention*, Springer, 2015, pp. 234–241.
- [3] K. He, G. Gkioxari, P. Dollár, and R. Girshick, "Mask r-cnn," in *Proceedings of the IEEE International Conference on Computer Vision (ICCV)*, Oct. 2017.
- [4] C. Yu, J. Wang, C. Peng, C. Gao, G. Yu, and N. Sang, "Bisenet: Bilateral segmentation network for real-time semantic segmentation," *CoRR*, vol. abs/1808.00897, 2018.
- [5] J. Hu, L. Li, Y. Lin, F. Wu, and J. Zhao, "A comparison and strategy of semantic segmentation on remote sensing images," in *The International Conference on Natural Computation, Fuzzy Systems and Knowledge Discovery*, Springer, 2019, pp. 21–29.
- [6] J. Aloimonos, I. Weiss, and A. Bandyopadhyay, "Active vision," *International journal of computer vision*, vol. 1, no. 4, pp. 333–356, 1988.
- [7] L. Hou, X. Chen, K. Lan, R. Rasmussen, and J. Roberts, "Volumetric next best view by 3d occupancy mapping using markov chain gibbs sampler for precise manufacturing," *IEEE Access*, vol. 7, pp. 121 949–121 960, 2019.
- [8] S. Isler, R. Sabzevari, J. Delmerico, and D. Scaramuzza, "An information gain formulation for active volumetric 3d reconstruction," in *Robotics and Automation (ICRA), 2016 IEEE International Conference on*, IEEE, 2016, pp. 3477–3484.
- [9] M. Brandão, R. Figueiredo, K. Takagi, A. Bernardino, K. Hashimoto, and A. Takanishi, "Placing and scheduling many depth sensors for wide coverage and efficient mapping in versatile legged robots," *The International Journal of Robotics Research*, vol. 39, no. 4, pp. 431–460, 2020.
- [10] J. Delmerico, S. Isler, R. Sabzevari, and D. Scaramuzza, "A comparison of volumetric information gain metrics for active 3d object reconstruction," *Autonomous Robots*, vol. 42, no. 2, pp. 197–208, 2018.
- [11] B. Yamauchi, "A frontier-based approach for autonomous exploration," in *Computational Intelligence in Robotics and Automation, 1997. CIRA'97., Proceedings., 1997 IEEE International Symposium on*, Jul. 1997, pp. 146–151.
- [12] S. Kriegel, C. Rink, T. Bodenmüller, and M. Suppa, "Efficient next-best-scan planning for autonomous 3d surface reconstruction of unknown objects," *Journal of Real-Time Image Processing*, vol. 10, no. 4, pp. 611–631, 2015.
- [13] S. M. LaValle, "Rapidly-exploring random trees: A new tool for path planning," 1998.
- [14] S. Karaman and E. Frazzoli, "Sampling-based algorithms for optimal motion planning," *The International Journal of Robotics Research*, vol. 30, no. 7, pp. 846–894, 2011.
- [15] A. Bircher, M. Kamel, K. Alexis, H. Oleynikova, and R. Siegwart, "Receding horizon" next-best-view" planner for 3d exploration," in *Robotics and Automation (ICRA), 2016 IEEE International Conference on*, IEEE, 2016, pp. 1462–1468.
- [16] —, "Receding horizon path planning for 3d exploration and surface inspection," *Autonomous Robots*, vol. 42, no. 2, pp. 291–306, 2018.
- [17] R. Mur-Artal and J. D. Tardós, "Orb-slam2: An open-source slam system for monocular, stereo, and rgb-d cameras," *IEEE Transactions on Robotics*, vol. 33, no. 5, pp. 1255–1262, 2017.
- [18] M. Bloesch, S. Omari, M. Hutter, and R. Siegwart, "Robust visual inertial odometry using a direct ekf-based approach," in *2015 IEEE/RSJ International Conference on Intelligent Robots and Systems (IROS)*, 2015, pp. 298–304.
- [19] S. Thrun, W. Burgard, and D. Fox, *Probabilistic robotics*. 2005.
- [20] H. Moravec and A. Elfes, "High resolution maps from wide angle sonar," in *Robotics and Automation. Proceedings. 1985 IEEE International Conference on*, IEEE, vol. 2, 1985, pp. 116–121.
- [21] S. Shah, D. Dey, C. Lovett, and A. Kapoor, "Airsim: High-fidelity visual and physical simulation for autonomous vehicles," in *Field and service robotics*, Springer, 2018, pp. 621–635.
- [22] N. Koenig and A. Howard, "Design and use paradigms for gazebo, an open-source multi-robot simulator," in *2004 IEEE/RSJ International Conference on Intelligent Robots and Systems (IROS)*, vol. 3, 2004, pp. 2149–2154 vol.3.
- [23] R. P. de Figueiredo, J. G. Hansen, J. L. Fevre, M. Brandão, and E. Kayacan, "On the advantages of multiple stereo vision camera designs for autonomous drone navigation," *CoRR*, vol. abs/2105.12691, 2021.